FEBS Letters

FEBS PRESS science publishing by scientists

Chemical effects on dye efflux activity in live zebrafish embryos and on zebrafish Abcb4 ATPase activity

Flavia Bieczynski[1,2], Kathleen Burkhardt-Medicke[2], Carlos M. Luquet[3], Stefan Scholz[2] and Till Luckenbach[2]

1 Centro de Investigaciones en Toxicología Ambiental y Agrobiotecnología del Comahue (CITAAC) – Consejo Nacional de Investigaciones Científicas y Técnicas (CONICET), Facultad de Ingeniería – Universidad Nacional del Comahue (UNCo), Buenos Aires, Neuquén, Argentina
2 Department Bioanalytical Ecotoxicology, Helmholtz Centre for Environmental Research – UFZ, Leipzig, Germany
3 Laboratorio de Ecotoxicología Acuática, Subsede INIBIOMA-CEAN (CONICET-UNCo), Junín de los Andes, Neuquén, Argentina

Correspondence
T. Luckenbach, Department Bioanalytical Ecotoxicology, Helmholtz Centre for Environmental Research – UFZ, Permoserstr. 15, 04318 Leipzig, Germany
Tel: +49-(0)341-235 1514
E-mail: till.luckenbach@ufz.de

Flavia Bieczynski and Kathleen Burkhardt-Medicke contributed equally to this article

(Received 15 July 2020, revised 9 October 2020, accepted 27 October 2020)

doi:10.1002/1873-3468.14015

Edited by Amro Hamdoun

ATP-binding cassette (ABC) transporter proteins include efflux pumps that confer multixenobiotic resistance to zebrafish embryos, a valuable toxico/pharmacological model. Here, we established an automated microscopy-based rhodamine B dye accumulation assay in which enhanced dye accumulation in live zebrafish embryos indicates inhibition of multixenobiotic efflux transporter activity. Twenty structurally divergent known substrates and/or inhibitors of human ABC transporters and environmentally relevant compounds were examined using this assay and the ATPase activity of recombinant zebrafish Abcb4 as readouts. These two assays confirmed that Abcb4 functions as an efflux transporter in zebrafish, whereas they gave discordant results for some of the tested substances. The dye accumulation assay in zebrafish embryos could be useful to screen environmental pollutants and other chemicals for efflux transporter interaction in a medium-throughput fashion.

Keywords: ABC efflux transporter; ATPase activity; chemosensitizer; dye accumulation assay; zebrafish Abcb4; zebrafish embryo

Aquatic species control the transition of chemicals from the water into the tissue through environment-tissue barriers, of which cellular transporter proteins are a component [1]. Members of the ATP-binding cassette (ABC) transporter protein family are highly important cellular efflux pumps that, concerning their substrates, are multispecific and confer so-called multixenobiotic resistance (MXR) that is equivalent to multidrug resistance (MDR) of cancer cells in chemotherapy [2–4]. Various ABC transporter orthologs conferring MXR were found to be expressed and active in fish [5,6]. Two P-glycoproteins were identified in the zebrafish genome, which first were designated *abcb1a* and *abcb1b*. Conversely, *abcb4* and *abcb5* were considered absent [7]. Later, synteny analyses revealed that *abcb1a* and *abcb1b* are indeed *abcb5* and *abcb4* orthologs, respectively, and that there is no *abcb1* ortholog in zebrafish [8,9]. Zebrafish Abcb4 is functionally homologous to human ABCB1 and acts as MXR efflux transporter [8,9]. Evidence of this has been obtained through different experimental approaches: (a) Morpholino knockdown of Abcb4 resulted in enhanced uptake of toxic or fluorescent human ABCB1 substrates (e.g., vinblastine and

Abbreviations
ABC, ATP-binding cassette; ATP, Adenosine triphosphate; bA, basal transporter ATPase activity; CAS, Chemical Abstracts Service; DMSO, dimethyl sulfoxide; hpf, hours post fertilization; KNIME, Konstanz Information Miner; Log P, octanol/water partition coefficient; LP sampler, large particle sampler; MS-222, ethyl 3-aminobenzoate methanesulfonic acid; MXR, multixenobiotic resistance; qRT-PCR, quantitative reverse transcription polymerase chain reaction; sA, stimulated transporter ATPase activity; VAST, vertebrate automated screening technology.

rhodamine B) by zebrafish embryos from the water; (b) upon exposure of zebrafish embryos to specific inhibitors of human ABCB1, such as PSC833, the uptake of ABCB1 substrates was enhanced, indicating inhibition of Abcb4-mediated efflux; and (c) human ABCB1 substrates and inhibitors readily interacted with zebrafish Abcb4 as corroborated by their stimulation or inhibition of the ATPase activity of recombinant Abcb4 protein [8]. This study provided also evidence for the localization of zebrafish Abcb4 in the epidermis, where it could mediate the efflux of chemicals from the embryo [8]. There is indication that ionocytes in the epidermis, which attain particularly high efflux transporter activity, may serve as gateways for the expulsion of chemicals from zebrafish embryos [10]. Although knockdown of zebrafish Abcb5 expression in the embryos did not indicate that this transporter mediates efflux of ABCB1 substrates from the embryo [8], high expression and activity of Abcb5 in ionocytes suggest that Abcb5 allows efflux of certain chemicals across the epidermis [10]. Fluorescent dyes acting as transporter substrates that are taken up from the water by aquatic animals can be used to visualize the action of MXR efflux transporters: Fluorescence of the tissue is low when the transporters are active, whereas it increases when the transporter function is reduced (e.g., ref. [3]). In the tissue of zebrafish embryos, the fluorescent dye rhodamine B increasingly accumulates when the MXR efflux transporter function is disrupted [8,11].

Compounds inhibiting the action of cellular efflux transporters and thereby enhancing the cellular sensitivity to toxic compounds are termed chemosensitizers [12,13]. By acting as chemosensitizers, a range of anthropogenic environmental compounds is assumed to have the potential to cause adverse ecotoxicological effects [14–16]. Fluorescent dyes that are efflux transporter substrates, such as rhodamine B, enable to determine the chemosensitizing potential of chemicals in native, live tissues of aquatic organisms; the chemosensitizing action of a test compound is indicated by increased dye accumulation in the tissue of interest [3,17].

In the study presented here, we developed a standardized assay for the quantitative measurement of the fluorescence of accumulated rhodamine B in the yolk sac of live zebrafish embryos. It thus is possible to determine the effects of chemical compounds on ABC efflux transporter activity in native tissue, thus eliminating both dye extraction steps for fluorometric measurements as in earlier protocols [8,11,18] and manual positioning of the embryo under the microscope [10]. This new protocol was first validated with cyclosporin A, verapamil, and MK571, which are standard efflux transporter inhibitors [6,19,20] that also interact with zebrafish Abcb4 (Fig. 2 F,L,S; [8]). Next, it was exploited to examine a range of chemicals, some with potential environmental relevance. Tested compounds comprised twelve drugs including known interactors of human ABCB1, five pesticides, two industrial compounds, and one fragrance compound. To explore the potential of this assay in full, the selected organic compounds were structurally diverse and covered a wide range of physicochemical properties (Table 1).

Dye accumulation data were correlated with data on the interaction of each compound with the zebrafish efflux transporter Abcb4. Compound–transporter interaction was determined by measuring the ATPase assays of recombinant zebrafish Abcb4 [21]. As the translocation of ABC transporter substrates is coupled to ATP hydrolysis [22,23], the ATPase activity provides an indication of chemical–transporter protein interaction [24].

The comparison between the chemical–efflux transporter protein interaction data obtained *in vivo* and *in vitro* allowed assessing Abcb4's contribution to the overall MXR transporter efflux activity in zebrafish embryos. By means of this new approach, we could gain insight into whether the effects of the tested compounds on Abcb4's ATPase assay are indicative of effects on efflux activity in whole embryos and to which degree an effect in the dye accumulation assay can be related to a chemical effect on Abcb4.

Materials and methods

Chemicals

Amprenavir, azinphos-methyl, bisphenol A, cyclosporin A, dipyridamole, ethyl 3-aminobenzoate methanesulfonic acid (MS-222), etoposide, ivermectin, metazachlor, phenanthrene, phenytoin, rhodamine B, thiacloprid, verapamil hydrochloride, and vinblastine sulfate were obtained from Sigma-Aldrich (Taufkirchen, Germany). Carbamazepine was purchased from Acros Organics/Thermo Fisher Scientific (Waltham, MA, USA), colchicine from Merck (Darmstadt, Germany), dexamethasone from AppliChem (Darmstadt, Germany), MK571 from Enzo Life Sciences Gmbh (Lörrach, Germany), tonalide from Bush Boake Allen Inc. (Montvale, NJ, USA), terbuthylazine from Riedel-de Haën (Seelze, Germany), and trospium from Selleckchem (Houston, TX, USA). For an overview with Chemical Abstracts Service (CAS) numbers, molecular weights, octanol/water partition coefficients (Log P), predicted water solubilities, and usages, refer to Table 1. For the experiments, stock solutions of the chemicals were set up in dimethyl sulfoxide (DMSO; 0.1% and 2% DMSO in the experimental solutions for the rhodamine B assays and

Table 1. Names, CAS numbers, molecular weights, log P, water solubilities (water sol.), and usage of the tested chemicals. Log*P* (KOWWIN v1.68 estimate) and water solubilities (WSKOW v1.42) were obtained with the EPI Suite software [54]. The SMILES codes of the compounds required for EPI Suite were retrieved from https://pubchem.ncbi.nlm.nih.gov/.

Chemical	CAS	MW	Log*P*	Water sol. (μM)	Usage
Amprenavir	161814-49-9	505.6	2.25	15.5	Protease inhibitor
Azinphos-methyl	86-50-0	317.3	2.75	65.9	Organophosphate insecticide
Bisphenol A	80-05-7	228.3	3.32	525.6	Industrial chemical
Carbamazepine	298-46-4	236.3	2.45	474.0	Anticonvulsant
Colchicine	64-86-8	399.5	1.30	1.1×10^5	Natural product
Cyclosporin A	59865-13-3	1202.6	1.00	0.002	Immunosuppressant
Dexamethasone	50-02-2	392.5	1.94	226.8	Glucocorticoid
Dipyridamole	58-32-2	504.7	2.74	6.1	Antiplatelet drug
Etoposide	33419-42-0	588.6	0.60	99.7	Topoisomerase inhibitor
Ivermectin	70288-86-7	875.1	4.61	3.1×10^{-4}	Macrocyclic lactone
Metazachlor	67129-08-2	277.8	2.13	1.5×10^3	Herbicide
MK571	115104-28-4	515.1	5.68	0.02	ABCC inhibitor, LTD4 antagonist
Phenanthrene	85-01-8	178.2	4.46	6.5	Industrial chemical
Phenytoin	57-41-0	252.3	2.47	126.8	Anticonvulsant
Terbuthylazine	5915-41-3	229.7	3.21	241.0	Herbicide
Thiacloprid	111988-49-9	252.7	2.33	917.6	Neonicotinoid insecticide
Tonalide (AHTN)	21145-77-7	258.4	5.70	4.8	Fragrance
Trospium chloride	10405-02-4	428	0.78	1036.0	Muscarinic antagonist
Verapamil hydrochloride	152-11-4	489.1	5.05	0.5	Calcium channel blocker
Vinblastine sulfate	143-67-9	907.1	2.52	0.11	Vinca alkaloid

the ATPase assays, respectively). Predicted water solubilities (Table 1) were used as orientation to set up the concentrations for the experiments. Higher experimental concentrations than predicted solubilities were used when no precipitation was visible in the solution. Rhodamine B stock solutions at 100 μM were prepared in Milli-Q water.

Maintenance of zebrafish and egg production

Zebrafish were maintained and bred according to standard protocols [25]. Collection of eggs and cultivation of embryos were performed as described elsewhere [26,27]. In short, fertilized eggs were separated from unfertilized eggs and incubated at 28 °C ± 1 in reconstituted water (294.0 $mg \cdot L^{-1}$ $CaCl_2$ $2H_2O$; 123.3 $mg \cdot L^{-1}$ $MgSO_4$ $7H_2O$; 63.0 $mg \cdot L^{-1}$ $NaHCO_3$; 5.5 $mg \cdot L^{-1}$ KCl [27]). Prior to use, this embryo culture water was aerated to reach oxygen saturation. All procedures followed the guidelines on the protection of experimental animals by the European Directive 2010-63-EU. Facilities for breeding and the production of embryos were licensed by the local government (Landesdirektion Leipzig, Aktenzeichen 75-9185.64).

Quantitative reverse transcription polymerase chain reaction (qRT-PCR)

Thirty zebrafish embryos at 72 h postfertilization (hpf) from three egg batches were added to Eppendorf tubes with 0.5 mL TRIzol Reagent (Invitrogen/Thermo Fisher Scientific, Waltham, MA, USA), homogenized, and total RNA was extracted according to the manufacturer. The extracts were treated with DNase I (Roche, Grenzach, Germany) to remove genomic DNA contamination. RNA integrity was verified using a NanoDrop Spectrophotometer (PEQLAB/VWR International GmbH, Darmstadt, Germany) and agarose gel electrophoresis. RNA concentrations in extracts were 1.1–1.2 $\mu g \cdot \mu L^{-1}$ cDNA, A260/A280 ratios were around 2, and A260/A230 ratios were 1.9–2.1. cDNA was synthesized from total RNA using RevertAid Reverse Transcriptase (200 $U \cdot \mu L^{-1}$; Fermentas/Thermo Fisher Scientific, Waltham, MA, USA) and random hexamer primers. Quantitative PCR was performed on a StepOnePlus PCR device (Applied Biosystems/Thermo Fisher Scientific, Waltham, MA, USA) using the SensiMix™ SYBR® Hi-ROX Kit (BioCat GmbH, Heidelberg, Germany). For qPCR primer sequences for zebrafish *abcb4* and *abcb5* and the housekeeping gene *ß-actin* and qPCR conditions, refer to Table S1. For qPCR data analysis, the amplification efficiency for target and housekeeping genes was set to 100%. Analysis of qPCR data was performed using the qgene core module (http://www.qgene.org/) [28,29].

Dye accumulation assay

The fluorescent dye rhodamine B, a substrate that first was found to be suitable as an indicator of human ABCB1 activity in dye accumulation assays [30], was used as a probe to measure the efflux transporter activity in the zebrafish embryo tissue. The compound increasingly accumulates in the embryo tissue when compounds inhibiting

Abcb4 activity are also present. The rhodamine B fluorescence levels in zebrafish embryos can thus serve as indirect measure of the Abcb4-mediated efflux transporter activity [8] although it needs to be considered that other cellular transporters can also mediate rhodamine B efflux. Dye accumulation assays were performed with hatched embryos at 72 hpf. This stage was selected, since the embryos were found to constitutively express *abcb4* transcript (refer to section "Expression of *abcb4* and *abcb5* transcripts in zebrafish embryos at 72 hpf" in the Results) and show efflux transporter activity (refer to Fig. 2) and manual dechorionation of the embryos is not necessary. Preparatory experiments served to test the experimental settings and parameters enabling to obtain clear rhodamine B fluorescence signals from tissue from control and inhibitor-treated embryos. Two sets of experiments were performed: Rhodamine B fluorescence levels were measured in the tissue of zebrafish embryos that were exposed (a) to 0.1, 0.5, or 1 μM rhodamine B without or with cyclosporin A (0.5–40 μM), a potent Abcb4 inhibitor ([8]; Fig. 3F), for 2 h (Fig. S2); (b) to 0.1 or 1 μM rhodamine B without or with cyclosporin A (10 μM) for 30 min to 4 h (Fig. S3). The results were evaluated for (a) a clear rhodamine B fluorescence signal and (b) a clear difference in rhodamine B fluorescence between inhibitor-treated and untreated embryos. Based on the results, dye accumulation assays with zebrafish embryos were performed in the following way: per control/treatment eight embryos were incubated for 2 h in a glass vial with 4 mL ISO water (28 °C, light-protected) with 1 μM rhodamine B either together with just the solvent (0.1% DMSO; negative control) or with 40 μM cyclosporin A (positive control) or in treatments with a test chemical at different concentrations. The maximum concentration of each test chemical was set according to its maximum water solubility (refer to Table 1). Treatments without rhodamine B and with test chemical only served to determine whether a fluorescence signal came from the chemical accumulated in the embryo tissue. The embryos were rinsed twice with ISO water upon incubations in the experimental solutions and transferred to the wells of a 96-well microplate (1 embryo per well) containing 200 μL ISO water with MS-222 (6 $g \cdot L^{-1}$) for anesthetization (refer to [31]). Per test chemical, dye accumulation assays were repeated at least once on separate days with embryos from different batches. For determining the amount of rhodamine B accumulated in the embryo tissue, each embryo was imaged at 535/590 nm (excitation/emission) and at bright field with a fluorescence microscope connected to the vertebrate automated screening technology (VAST) system in an automated way (see below). The time span from when the exposures were terminated to the onset of the fluorescence measurements in the VAST system was approximately 10 min. Per control/treatment eight embryos were imaged. Prior to imaging, each embryo was inspected for showing heartbeat and for being morphologically intact.

Fluorescence and bright-field imaging of fish embryos

The VAST BioImager platform (Union Biometrica, Geel, Belgium) in combination with the large particle sampler (LP sampler; Union Biometrica) and a Leica fluorescence microscope (Leica DM6B equipped with a Leica Digital Camera DFC 365FX; Leica Microsystems, Wetzlar, Germany) with a 5× objective was used to take fluorescence and bright-field images of the live, anesthetized embryos upon exposures to test chemicals and rhodamine B (Fig. 1). The setup was designed to automatically load a single embryo from a microplate into a glass capillary located in front of a microscope lens, position the embryo, take images of the embryo with predetermined parameters (magnification and region of the embryo that is imaged, fluorescence and/or bright-field images, exposure time, brightness of the illumination), and expulsion of the embryo from the glass capillary into a beaker. For imaging, each embryo was automatically positioned in a lateral orientation. Imaging was performed at maximum excitation light intensity. Fluorescence images of the predetermined embryo region were obtained with 50, 100, 200, and 400 ms of exposure to confirm that the increase in the fluorescence signal was linear with longer exposure times. The exposure time of 50 ms proved to be sufficiently sensitive to capture the fluorescence signal, which was in the range of linear increase in the fluorescence signal with exposure time (see below). Therefore, from the experiments with the test compounds only the images obtained with 50 ms exposure time were analyzed.

The duration of the procedure comprising loading, positioning, imaging, and expulsion of each embryo from the capillary was around 90 s per embryo. Depending on the number of embryos, the time period between the capture of the images of the first and the last embryo on a microplate was around 150 min. Hence, each embryo remained for a different time span in the plate prior to the measurement. The plate layout was arranged to avoid a potential plate position bias on the fluorescence quantification. However, it was not observed that the fluorescence tissue levels in the embryos decreased over the time that they were kept in the multiwell plate prior to imaging. In a pre-experiment, fluorescence was measured in embryos that were kept in control medium for different periods of time after exposure to rhodamine B and cyclosporin A. Fluorescence levels in the embryo tissue were not significantly changed after 3 h but reached almost 0 after 18 h, indicating slow clearance of the embryo tissue from rhodamine B (refer to Fig. S4).

Quantification of fluorescence intensity

The fluorescence intensity as a proxy of the rhodamine B amount accumulated in the zebrafish embryo tissue was determined by quantifying the brightness of a predefined

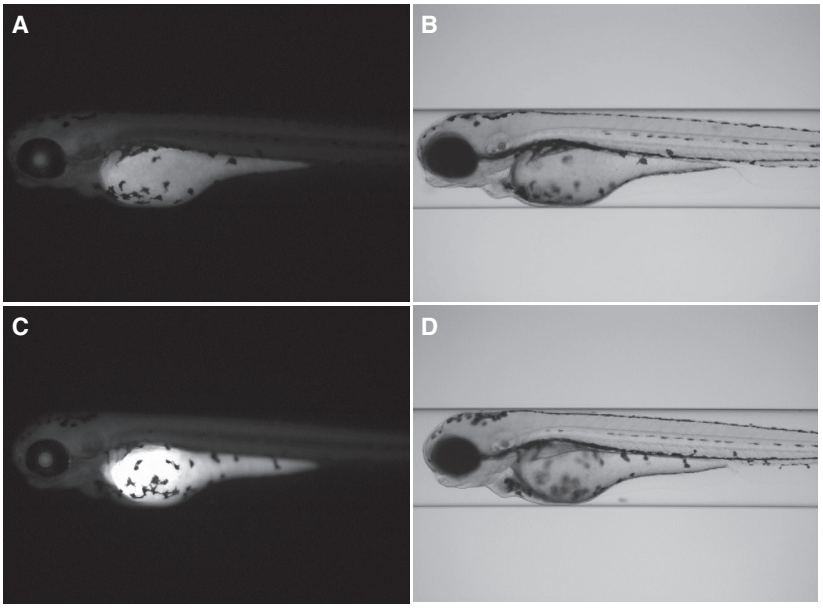

Fig. 1. Fluorescence (A, C) and bright-field (B, D) images of live zebrafish embryos upon exposure to rhodamine B at 1 μM for 2 h. For imaging, the embryos were automatically positioned in lateral orientation in glass capillaries using the VAST system. (A, B) Solvent control (0.1% DMSO); (C, D) cyclosporin A (40 μM) treatment.

area (220 × 100 pixels, corresponding to 1.3 × 0.59 mm^2) in the yolk region (Fig. S1). The process of automatically selecting the predefined area and of determining its brightness was operated with the Konstanz Information Miner (KNIME) analytical platform (Version 3.5.3. [32]). The KNIME workflow is provided in the Supporting Information.

Zebrafish Abcb4 ATPase assays

The ATPase assays with recombinant zebrafish Abcb4 were performed as described in Refs [8,21]. Briefly, recombinant Abcb4 protein was generated using the baculovirus expression system. The ATPase assays were performed in 96-well plates enabling simultaneous incubations of treatments with various concentrations of the test compounds and controls. The test compounds were dissolved in DMSO, and the stocks were diluted 1 : 50 (2% DMSO in the experimental solutions and in the controls). In parallel, negative controls ('basal transporter ATPase activity', bA) and positive controls with 40 or 50 μM verapamil were run. The effects of both 40 and 50 μM verapamil were in the upper plateau range of the sigmoidal regression curve (Fig. 3S), indicating maximum stimulation of the transporter ATPase activity by verapamil at these concentrations ('stimulated transporter ATPase activity', sA).

Analyses of transporter activity data

All data obtained with the dye accumulation (arbitrary fluorescence units) and the ATPase assays (enzyme activity as nmol $P_i \times \min^{-1} \times$ mg membrane protein^{-1}) were transformed into percentage values. The data from the negative controls (only solvent; 0.1% or 2% DMSO) run in parallel in an experiment were set to 100%. For analysis of the data from the test on inhibition of the stimulated Abcb4 ATPase, data were also related to respective stimulated ATPase activities (sA) that were set to 100%. Concentration–response relationships of the data were described with the nonlinear four-parameter HILL model:

$$R(c_t) = min + \frac{(max - min)}{1 + (\frac{EC50}{c_t})^p} \quad (1)$$

where $R(c_t)$ is the fluorescence or P_i levels relative to controls (in %) in treatments at a certain concentration of the test compound (c_t); *min* is the fluorescence level of the controls in the dye accumulation assay, bA in the ATPase test for stimulation and estimated in the ATPase test for inhibition; *max* is the maximum fluorescence level in the dye accumulation assay (estimated) and the maximum ATPase activity in the test for ATPase stimulation (estimated) and for ATPase inhibition (set to sA); c_t is the concentration of test compound (t); p is the HILL number; and $EC50$ is the parameter value describing the concentration of inhibitor causing 50% of the maximal effect.

If a regression could not be fitted to the data with the HILL model, linear regression was used.

If the HILL model could be fitted, this was taken as indication for clear effects of the test compound in the respective test. If linear regression was used to model the data from the rhodamine B accumulation assay and the slope was positive, this was interpreted as indication for slight effects by the test compound.

For correlation analyses of the effect levels of the different assays, Pearson's correlation coefficients were

calculated. For each tested compound, the maximum experimentally determined effect levels in each test were determined. All analyses were computed with GraphPad Prism 8 for macOS (GraphPad Software, San Diego, CA, USA).

Results

Expression of *abcb4* and *abcb5* transcripts in zebrafish embryos at 72 hpf

We initially sought to determine the expression levels of *abcb4* and *abcb5* transcripts in zebrafish embryos at 72 hpf. Mean (±SD) relative constitutive expression levels normalized to *ß-actin* were 3.2×10^{-3} ($\pm 0.2 \times 10^{-3}$) for *abcb4* and 12.5×10^{-3} ($\pm 0.2 \times 10^{-3}$) for *abcb5* transcripts in zebrafish embryos at 72 hpf (refer to Table S1 for the respective cycle threshold (C_t) values in the qPCR).

Method evaluation—rhodamine B accumulation in zebrafish embryos

Fluorescence images of zebrafish embryos exposed to rhodamine B showed a bright signal in the yolk sac (Fig. 1A,C), indicating that the dye taken up from the water is mainly accumulated in the yolk. In embryos exposed to a combination of rhodamine B and cyclosporin A, the fluorescence signal was clearly brighter, indicating enhanced accumulation of rhodamine B in the yolk (Fig. 1C). In pilot experiments, rhodamine B concentration and exposure times were evaluated to obtain robust and clear fluorescence signals above the background with a linear increase in signal intensity (Figs S2 and S3). Arbitrary fluorescence levels ranged approximately from 1 to 8 at 0.1 μM rhodamine B, from 5 to 40 at 0.5 μM rhodamine B, and from 8 to 50 at 1 μM rhodamine B (Fig. S2). The fluorescence levels in control and in cyclosporin A co-treated embryos increased linearly with the exposure time; the differences between control and treated embryos were similar at the different time points (Fig. S3). To obtain robust fluorescence signals, we decided to employ 1 μM rhodamine B in all subsequent experiments and to expose the embryos in the experimental solutions for 2 h prior to imaging.

Effects of test compounds on rhodamine B accumulation in zebrafish embryos

Clear increases in rhodamine B fluorescence in zebrafish embryos were seen for ten of the 20 tested compounds, which were azinphos-methyl, carbamazepine, cyclosporin A, dipyridamole, ivermectin, metazachlor, MK571, terbuthylazine, tonalide, and verapamil. For all of those compounds, the concentration-dependent changes in fluorescence could be described with the HILL model (Eqn 1; Fig. 2B,D,F,H,J,K,L,O,Q,S; Table 2). The maximum fluorescence changes were 1.6-fold (carbamazepine, Fig. 2D) to 3.5-fold (cyclosporin A, Fig. 2F). Slight fluorescence increases were found for phenanthrene (Fig. 2M) and vinblastine (Fig. 2T; positive slopes, Table 2); slight fluorescence decreases occurred with bisphenol A (Fig. 2C) and phenytoin (Fig. 2N; negative slopes, Table 2). The rest of the compounds showed no effect on rhodamine B fluorescence in the embryos (Fig. 2). The fluorescence levels in relation to the concentrations of the compounds causing slight or no effects were described with linear regression (Fig. 2A,C,E,G,I,M,N,P,R,T).

Effects of test compounds on Abcb4 ATPase activity *in vitro*

Zebrafish Abcb4 ATPase activity was maximally stimulated up to almost fourfold by amprenavir (Fig. 3A), followed by verapamil with 3.3-fold stimulation at maximum (Fig. 3S).

Maximum Abcb4 ATPase stimulation was > twofold by five compounds in the order amprenavir > verapamil > cyclosporin A > azinphos-methyl > dipyridamole. Concentration-dependent Abcb4 ATPase stimulation by these compounds could be described with the nonlinear HILL regression (Eqn 1; Fig. 3A,B,F,H, S). In addition, the concentration-dependent stimulations by dexamethasone (1.7-fold maximum stimulation; Fig. 3G) and vinblastine (1.3-fold maximum stimulation; Fig. 3T) followed the HILL model. Ivermectin and MK571 had a concentration-dependent inhibiting effect on the basal Abcb4 ATPase activity that also followed the HILL model (Fig. 3J,L). For all other compounds, linear regression was applied. Compounds causing slight stimulation of the basal ATPase activity were etoposide, metazachlor, terbuthylazine, thiacloprid, and trospium (Fig. 3I,K,O,P,R). Slight inhibitions of the basal ATPase activity were seen with bisphenol A (Fig. 3C), carbamazepine (Fig. 3D), colchicine (Fig. 3E), phenanthrene (Fig. 3M), and tonalide (Fig. 3Q; for regression parameters, refer also to Table 2).

Most of the tested compounds had inhibitory effects on the stimulated Abcb4 ATPase (Fig. 3). Bisphenol A and ivermectin had the most pronounced effects, resulting in 35% and 39% of the respective basal ATPase activities, respectively (Fig. 3C,J). When the ATPase activities in the bisphenol A and ivermectin treatments causing the highest effects were related to

Table 2. Parameters of nonlinear HILL (Eqn 1) or linear regressions performed with the concentration–effect data retrieved with the dye accumulation and zebrafish Abcb4 ATPase assays.

	Dye accumulation assay					ATPase assay					
	Linear regression		Nonlinear regression				Linear regression		Nonlinear regression		
Chemical	Slope	r^2	Hill slope	EC50 (μM)	r^2	ATPase -	Slope	r^2	Hill slope	EC50 (μM)	r^2
Amprenavir	0.08	3E-05				Inhibition					
						Stimulation			0.575	~ 6118	0.94
Azinphos-methyl			2.58	21.9	0.68	Inhibition	19.01	0.08			
						Stimulation			0.9292	160.5	0.69
Bisphenol A	-5.14	0.34				Inhibition			2.4×10^{14}	~ 0.014	-0.12
						Stimulation	-9.12	0.13			
Carbamazepine			2.88	184.7	0.57	Inhibition	-2.22	0.01			
						Stimulation	-2.90	0.01			
Colchicine	-2.87	0.03				Inhibition			-1.125	27.47	0.65
						Stimulation	-5.19	0.07			
Cyclosporin A			1.00	3.32	0.75	Inhibition			-0.15	~ 4.7×10^{11}	0.52
						Stimulation			0.60	0.04	0.29
Dexamethasone	2.62	0.01				Inhibition			-0.19	609.9	0.21
						Stimulation			0.51	17.22	0.29
Dipyridamole			1.25	6.4	0.33	Inhibition					
						Stimulation			0.71	0.27	0.21
Etoposide	0.99	0.00				Inhibition	22.26	0.19			
						Stimulation	3.03	0.20			
Ivermectin (mainly b1A)			1.54	0.65	0.72	Inhibition			-0.33	618	0.30
						Stimulation			-0.61	91.44	0.01
Metazachlor			1.08	60.34	0.87	Inhibition	0.18	0.06			
						Stimulation	10.35	0.16			
MK571			1.52	~ 3432	0.90	Inhibition			-0.61	53.17	0.11
						Stimulation			-1.26	4.48	0.15
Phenanthrene	11.24	0.19				Inhibition			-2.31	0.07	0.07
						Stimulation	-6.23	0.12			
Phenytoin	-7.45	0.16				Inhibition			-0.31	120.4	0.11
						Stimulation	4.41	0.25			
Terbuthylazine			0.67	90.18	0.98	Inhibition	4.09	0.02			
						Stimulation	15.65	0.45			
Thiacloprid	5.66	0.108				Inhibition			-0.52	1118	0.58
						Stimulation	20.06	0.23			
Tonalide (AHTN)			~ 16.78	~ 5.42	0.75	Inhibition			-1.09	51.74	0.37
						Stimulation	-11.32	0.12			
Trospium chloride	-0.59	0.002				Inhibition			-0.62		
	0.03	0.17									
						Stimulation	0.11	0.20			
Verapamil hydrochloride			1.41	39.81	0.93	Inhibition					
						Stimulation			0.91	3.12	0.54
Vinblastine sulfate	4.77	0.043				Inhibition			-0.53	14.54	0.60
						Stimulation			1.18	0.85	0.09

the respective stimulated ATPase activities, the effects were 90% and 88% inhibition, respectively. Strong inhibiting effects of the ATPase activity were also seen by cyclosporin A, vinblastine, MK571, etoposide, tonalide, and phenanthrene (Fig. 3F,I,L,M,Q,T). When the ATPase activities in the respective treatments with these compounds were related to the respective stimulated ATPase activities, the resulting effects equaled 60–76% inhibition. The other compounds showed between 20% and 56% inhibition or, for azinphos-methyl, metazachlor, and terbuthylazine, slight increases in the activated ATPase activities (Fig. 3B,K,O; refer also to Table 2). The concentration–effect relationships for bisphenol A, cyclosporin

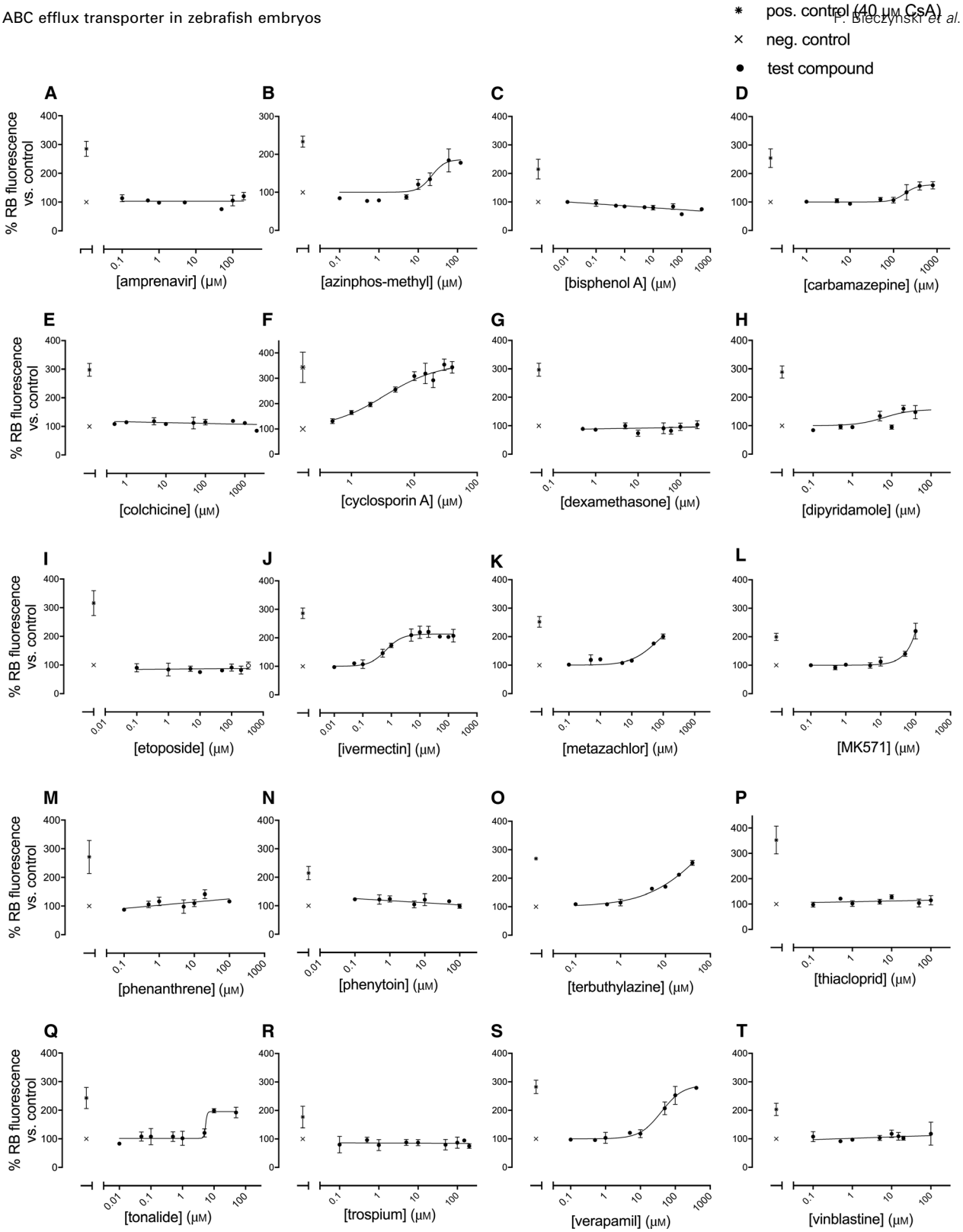

Fig. 2. (A–T) Fluorescence levels in zebrafish embryos upon incubation to 1 µM rhodamine B along with chemicals at different concentrations for 2 h. The percentage fluorescence relative to the respective control (0.1% DMSO) was plotted vs. chemical concentration. Symbols and bars represent means ± SE. Data points are from 2 to 6 replicates; each replicate is the mean fluorescence measured in eight embryos exposed and measured on the same day. Cyclosporin A (40 µM) was tested in each experimental series as positive control; exposures with rhodamine B along with 0.1% DMSO served as negative controls. Data were fitted with linear or nonlinear regression (HILL model, Eqn 1). For regression parameters, refer to Table 2.

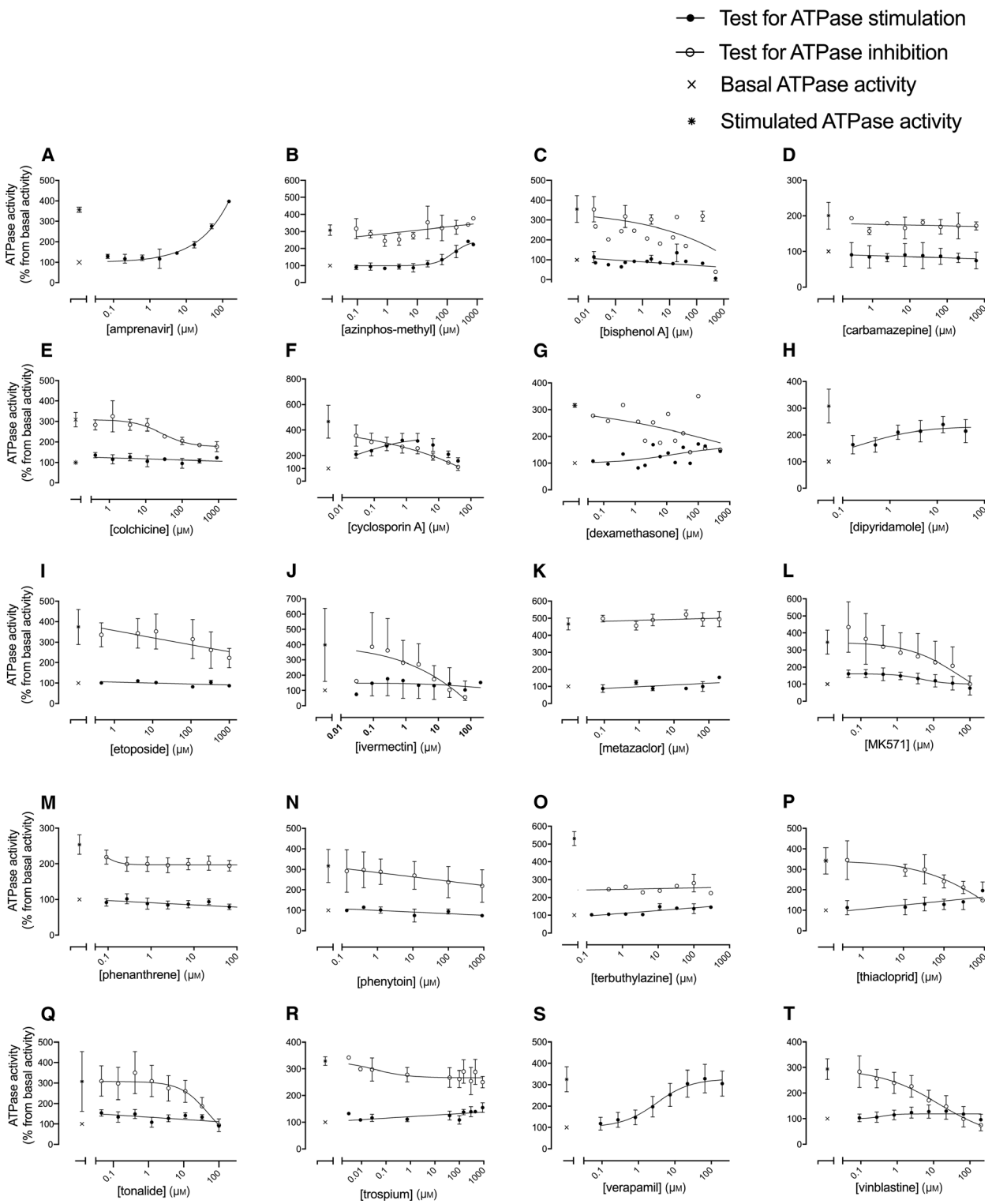

Fig. 3. (A–T) ATPase activities of recombinant zebrafish Abcb4 protein in the presence of chemicals at different concentrations. The percentage ATPase activity relative to the respective control (2% DMSO) was plotted vs. chemical concentration. Symbols and bars represent means ± SE from 1 to 5 replicates. All compounds were tested for stimulation of the basal Abcb4 ATPase activity; most compounds were also tested for inhibition of the Abcb4 ATPase activity stimulated with 40 or 50 μM verapamil. Verapamil (40 or 50 μM) was tested in each experimental series as positive control (stimulated activity; sA); reactions with 2% DMSO served as negative controls (basal activity; bA). Data were fitted with nonlinear (HILL model, Eqn 1) or linear regression. For regression parameters, refer to Table 2.

A, dexamethasone, ivermectin, MK571, phenanthrene, phenytoin, thiacloprid, tonalide, trospium, and vinblastine could be described with the HILL model (Fig. 3C,F,G,J,L,M,N,P,Q,R,T). For the other compounds, linear regression was applied (Fig. 3, Table 2).

Correlation of the test compounds' effects on rhodamine B accumulation and ATPase activity

Correlation analyses of the maximally measured effect levels were performed to compare the effects of the test compounds in the different assays (Fig. 4A–C).

To correlate the chemical effects on the basal (bA; test for ATPase stimulation) and the stimulated Abcb4 ATPase activities (sA; test for ATPase inhibition), effect data of the stimulation tests were related to the bA and of the inhibition tests to the respective sA. The ATPase stimulation and inhibition effects did not show a significant correlation ($P > 0.05$; Fig. 4A). The data points of more than half of the compounds in the analysis were outside the 95% confidence intervals of the linear regression (slope = −0.07; $r^2 = 0.04$). The linear regression curve line intersects the 100% level (i.e., point of no effect) on the ATPase stimulation axis at the point of 54% (i.e., decrease to 54% of the stimulated ATPase activity) on the ATPase inhibition axis (Fig. 4A). This concurs with the finding that stimulation and inhibition effects did not correlate. For two compounds, cyclosporin A and metazachlor, both pronounced stimulating and inhibiting effects were found. The data points of these compounds were close to the regression line, as were the data points of thiacloprid, dexamethasone, terbuthylazine, and phenanthrene. The data point of phenanthrene, which did not cause ATPase stimulation but ATPase inhibition, was next to the intersection point of the linear regression line with the 100% (i.e., control) level on the stimulation axis. Etoposide, vinblastine, and bisphenol A elicited pronounced ATPase inhibiting but no ATPase-stimulating effects, similar to phenanthrene. Only azinphos-methyl caused pronounced ATPase stimulation but rather weak inhibition of the stimulated Abcb4 ATPase activity. Both no or weak stimulation and inhibition of the Abcb4 ATPase were elicited by carbamazepine, phenytoin, trospium, and colchicine (Fig. 4A).

The chemical effects on the accumulation of rhodamine B in live embryos correlated significantly with the stimulatory effects of the test compounds on Abcb4 ATPase activity *in vitro* ($P < 0.05$; Fig. 4B). Although the data points for most of the tested compounds were outside the 95% confidence intervals of the linear regression analysis (slope = 0.25; $r^2 = 0.27$), most of the data points were relatively close to the confidence interval limits. The data points obtained with compounds that caused no or only slight effects on dye accumulation ranged from a 10% (etoposide) to 71% (dexamethasone) effect in the ATPase stimulation assay. This, in addition to the data point of amprenavir, the only compound that caused a strong Abcb4 ATPase stimulation but only a small effect in the dye accumulation assay can be seen as a reason for the regression line intersecting the 100% level (no effect on dye accumulation) on the rhodamine B fluorescence axis at 145% (i.e., 45% above control) on the ATPase stimulation axis (Fig. 4B).

Conversely, the chemical effects on rhodamine B fluorescence in zebrafish embryos did not significantly correlate with the inhibitory effects on stimulated Abcb4 ATPase activity ($P > 0.05$; Fig. 4C). The data points of about half of the compounds were outside the 95% confidence intervals of the linear regression analysis (slope = −0.09; $r^2 = 0.08$). The regression line intercepted the 100% level (no effect on dye accumulation) on the rhodamine B fluorescence axis at 58% (i.e., 42% effect on ATPase inhibition) on the Abcb4 ATPase inhibition axis (Fig. 4C). The compounds causing pronounced effects in both tests comprised cyclosporin A, metazachlor, ivermectin, MK57, and terbuthylazine. A range of compounds, including trospium, phenytoin, colchicine, dexamethasone, thiacloprid, phenanthrene, etoposide, vinblastine, and bisphenol A, caused no or only comparatively weak effects on rhodamine B accumulation; on the ATPase inhibition axis, the scatter of these compounds was relatively wide, ranging from 76.7% (23.3% effect) for trospium to 10.2% (89.8% effect) for bisphenol A. Carbamazepine and azinphos-methyl caused comparatively little decreasing effects on the stimulated Abcb4 ATPase activity but pronounced effects on rhodamine B accumulation in zebrafish embryos (58% and 84%, respectively, above control).

Discussion

We here present a new approach that allows performing dye accumulation assays in zebrafish embryos and quantification of the fluorescence as a measure of the accumulated dye in the live embryos using a fluorescence microscope connected to the VAST system for automatic loading, positioning, and imaging of the embryo. In this way, the fluorescence can be directly analyzed in living, intact embryos, avoiding a potential bias caused by additional steps, such as the extraction of the dye from the tissue. The automated positioning of the embryo in front of the microscope lens avoids

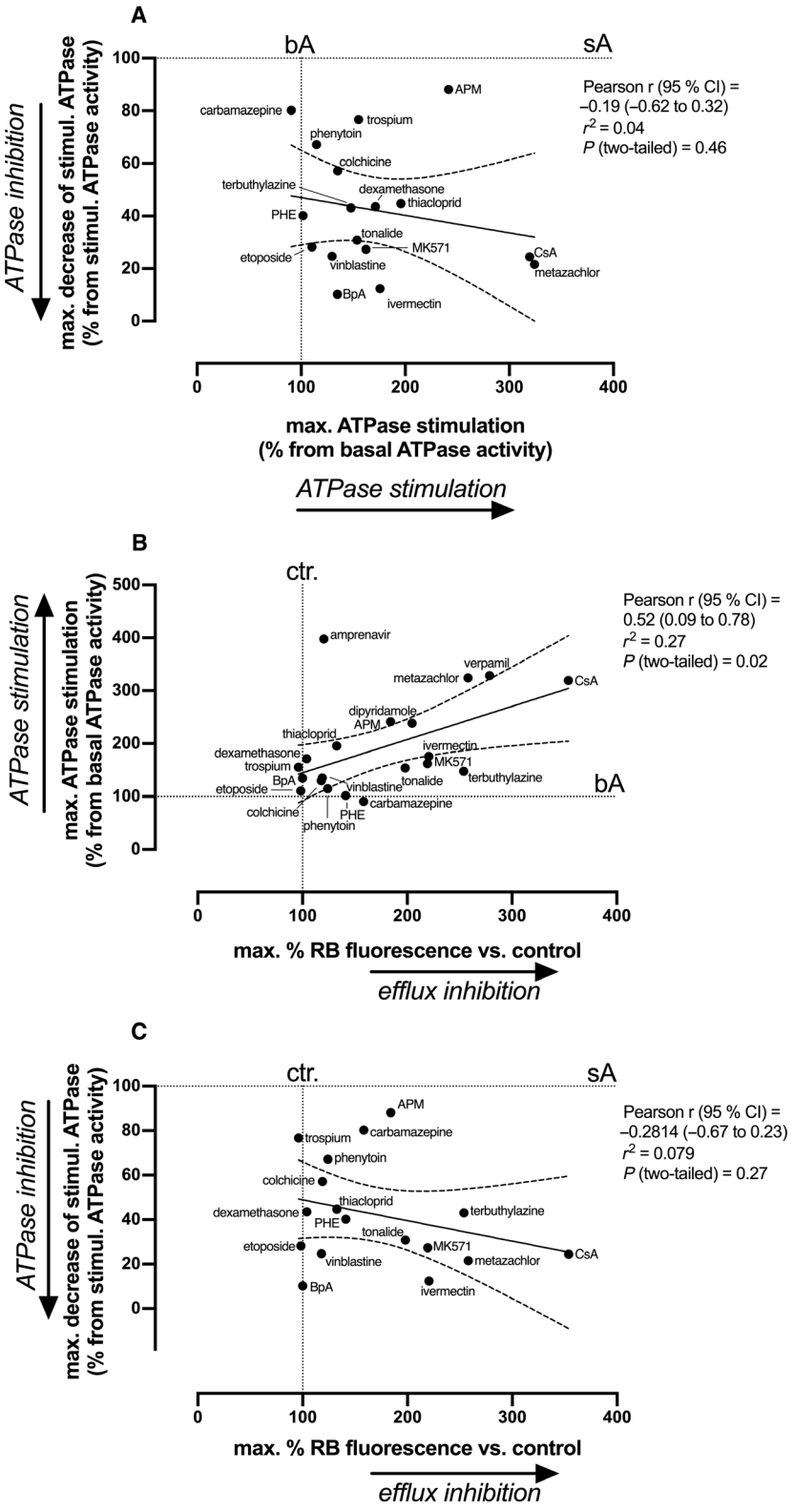

Fig. 4. (A–C) Correlations of the maximum measured effect levels for each compound in the different tests: (A) maximum inhibition of stimulated Abcb4 ATPase activity vs. the maximum stimulation of the basal Abcb4 ATPase activity; (B) maximum stimulation of the basal Abcb4 ATPase activity vs. the maximum observed increase in fluorescence in the dye efflux assay; and (C) maximum inhibition of stimulated Abcb4 ATPase activity vs. the maximum observed increase in fluorescence in the dye efflux assay. Each compound is represented by a data point. Pearson's correlation parameters are shown in the respective graphs. Linear regressions are with 95% confidence intervals. APM, azinphos-methyl; bA, basal ATPase activity; BpA, bisphenol A; CsA, cyclosporin A; ctrl, control; PHE, phenanthrene; sA, stimulated ATPase activity. Equations for linear regressions are as follows: (a) $y = -0.06692x + 53.66$; (b) $y = 0.6272x + 82.25$; and (c) $y = 0.09262x + 58.07$.

variability that could arise from the operator. As the imaging procedure is automated and thus streamlined, this dye accumulation assay can be performed in a standardized fashion and with a medium throughput.

Zebrafish embryos are important model systems in toxicological and pharmacological research [33–35]; knowledge about interaction of test compounds with efflux transporter activity can be essential for an understanding of the toxico/pharmacokinetics of test compounds in the zebrafish embryo. The approach of using live and intact zebrafish for studying chemical effects on efflux transporter activity has the advantage that all processes that are relevant for chemical efflux activity in the embryos are considered.

The accumulation of rhodamine B in the yolk served as indicator for efflux transporter activity in the embryo. The yolk in the zebrafish embryo is the main site where rhodamine B accumulates. A range of proteins are expressed in the yolk syncytial layer (YSL) that drive translocation processes of biological molecules [36], and it is conceivable that the activity of such transporter proteins leads to the accumulation of rhodamine B in the yolk. Accumulation of rhodamine B in the yolk is enhanced if efflux transporter activity is disrupted (Fig. 1). Our qPCR data confirm the presence of *abcb4* and *abcb5* transcripts in 72 hpf zebrafish embryos (see above) , which is the developmental stage used here in the dye accumulation assays. This can be seen as indication for the expression also of Abcb4 and Abcb5 protein. Relative *abcb5* transcript levels were approximately fourfold higher than those of *abcb4*. Although there is indication that zebrafish Abcb5 mediates efflux of xenobiotics from zebrafish embryos [10] and the human ABCB5 ortholog was shown to act as multidrug transporter [37], Abcb5 action does not visibly modify accumulation of rhodamine B in zebrafish embryos. Thus, knockdown of Abcb5 expression does not result in modified accumulation of rhodamine B in the embryo tissue [8]. It therefore can be excluded that inhibition of zebrafish Abcb5 by test chemicals has an effect on rhodamine B accumulation in the embryos.

Further evidence for the presence and function of Abcb4 in 72 hpf zebrafish embryos comes from experiments showing enhanced rhodamine B accumulation in the yolk of the embryos when known Abcb4 inhibitors ([8]; see below) were also present. The co-exposure of 72 hpf embryos to Abcb4 inhibitors led to enhanced accumulation of rhodamine B in the yolk (Figs 1 and 2), indicating Abcb4-mediated rhodamine B efflux also in this stage. A function of Abcb4 as efflux transporter of rhodamine B in zebrafish embryos was shown previously: Disruption of Abcb4 function by knockdown or chemical inhibition leads to enhanced rhodamine B accumulation in the yolk, indicating that Abcb4 prevents the diffusion of this dye into the yolk [8]. In addition to Abcb4, also other cellular transporter types may contribute to the overall cellular efflux activity in zebrafish embryos (see below).

A range of structurally diverse chemicals was examined in this study for their interaction with efflux transporter activity using live zebrafish embryos and a recombinant zebrafish efflux transporter protein. The test compounds comprised known interactors of human ABCB1, such as amprenavir, colchicine, cyclosporin A, dexamethasone, dipyridamole, etoposide, ivermectin, trospium, verapamil, and vinblastine [38–42]. Carbamazepine and phenytoin were shown not to interact with human ABCB1 [40,43]. Only four of those ten compounds, cyclosporin A, dipyridamole, ivermectin, and verapamil, showed clear effects in the dye accumulation assay in this study, leading to enhanced rhodamine B accumulation in the tissue used as indication for the inhibition of rhodamine B efflux (Fig. 2F,H,J,S). However, in the ATPase assays, all of those compounds caused stimulation and/or inhibition of the Abcb4 ATPase (Fig. 3A,E,F,G,H,I,J,R,S,T), indicating interaction of those compounds with zebrafish Abcb4. On the other hand, carbamazepine, in agreement with the results with human ABCB1, did not elicit the effects on the Abcb4 ATPase activity (Fig. 3D) but enhanced dye accumulation in the embryos, indicating disrupted dye efflux (Fig. 2D). Of the 20 compounds tested here, seven—azinphosmethyl, cyclosporin A, dipyridamole, ivermectin, MK571, tonalide, and verapamil—showed clear effects on both dye accumulation and ATPase activity, that is, data in both tests could be fitted with the HILL model. Phenanthrene, thiacloprid, and vinblastine showed slight effects in the rhodamine B uptake assay (Fig. 2M,P,T; linear regression slope > 4, Table 2) and clear (thiacloprid, vinblastine) or slight effects (phenanthrene) in the ATPase assay. Discrepancies in the results of the dye accumulation and ATPase assays for several compounds are mirrored by the correlation analyses of maximum effect levels in the different assays: Although a moderate correlation of the results from the dye accumulation and ATPase stimulation assays was found, there were clear exceptions that did not fit to this correlation, such as for amprenavir and terbuthylazine (Fig. 4B); no significant correlation was found for the results from the dye accumulation and ATPase inhibition assays (Fig. 4C). As it was unambiguously indicated earlier that zebrafish Abcb4 is an efflux transporter of rhodamine B in embryos [8], the following reasons are conceivable why dye

accumulation and ATPase stimulation/inhibition assay results do not coincide in several cases, as found in this study:

1 Rhodamine B efflux in live zebrafish embryos is, in addition to Abcb4, also mediated by the activity of other cellular transporters. So far, indications were obtained for expression of Abcc1, Abcc2, and multidrug and toxin extrusion (MATE) proteins in zebrafish embryos at 72 hpf [44–47]. This could explain why certain compounds, such as carbamazepine or terbuthylazine, exerted clear effects in the dye accumulation assay but no or slight effects in the ATPase stimulation/inhibition assays.
2 For cases when test compounds caused clear effects in Abcb4 ATPase stimulation/inhibition assays but slight or no effects in the dye accumulation assay, it is conceivable that the test compounds did not compete with rhodamine B for binding sites in the protein. Thus, it was earlier proposed that human ABCB1 has at least two substrate-binding sites [48–50] and there is more recent evidence for a large, flexible cavity in the transmembrane domain of ABCB1, holding several sites to which chemicals bind [51,52]. Thus, rhodamine B efflux by zebrafish Abcb4 may only be sensitive for certain compounds interacting with the protein.
3 A further aspect that should be considered is accessibility of the rhodamine B mediating efflux transporter in zebrafish embryos to test compounds. It is striking that clear effects in the dye accumulation assay were seen for compounds with $log\ P > 3$, that is, the more lipophilic compounds. These included ivermectin, MK571, phenanthrene, terbuthylazine, tonalide, and verapamil (Fig. 2J,L,M,Q,S; Table 1). In contrast, many, more hydrophilic compounds ($log\ P < 2$), such as colchicine, dexamethasone, etoposide, and trospium (Fig. 2E,G,I,R; Table 1), elicited no or only slight effects in the dye accumulation assay. This may be related to a generally higher concentration of the more lipophilic compound molecules in cellular membranes and at the transporter proteins. This relation of lipophilicity and effect in the assay does not apply for cyclosporin A, a hydrophilic compound causing a strong effect in the dye accumulation test (Fig. 2F, Table 1), and for the comparatively lipophilic bisphenol A, causing no increased dye accumulation in the embryos (Fig. 2C, Table 1). For those compounds, either comparatively few molecules are sufficient for pronounced effects, as the compound interacts in comparison strongly with the efflux transporter proteins (cyclosporin A); contrariwise, there is little interaction with the efflux transporters by the test compound, so that also high concentrations of the compound do not cause effects (bisphenol A).

About half of the test compounds with environmental relevance, comprising—in addition to the known ABCB1 interactors ivermectin and verapamil—azinphos-methyl, bisphenol A, metazachlor, phenanthrene, terbuthylazine, thiacloprid, and tonalide, showed effects in the dye accumulation or in the ATPase assays or in both tests (Figs 2 and 3; Table 2). This confirms the notion that interaction of anthropogenic, environmentally relevant chemicals with cellular MXR efflux transporters may be quite common [3], and indeed, as it was phrased for pharmaceuticals [53], it may be an exception if no interaction by an environmental chemical with cellular transporters occurs.

Conclusions

Our study was performed with a relatively small number of test compounds; however, it nevertheless provides some important insights into the interaction of structurally diverse chemicals with cellular efflux transporter activity in zebrafish embryos. A comparison of the results of the two assays indicates that disruption of zebrafish Abcb4 by interaction with several of the test compounds leads to reduced efflux activity in the zebrafish embryo. However, it appears that the results from the different assays are only partially related, that is, results from the Abcb4 ATPase assay cannot be directly translated to the general efflux transporter activity in the whole embryo. Conceivable reasons are as follows: (a) Other transporters than Abcb4 also mediate efflux of chemicals in the zebrafish embryo; (b) interaction of a test compound with the efflux transporter protein in the zebrafish embryo may not always lead to competitive inhibition of efflux of the proxy dye; and (c) the accessibility of transporter proteins to test compounds differed in the different test systems. Further research is necessary to address these aspects: (a) Analyses of chemicals in the tissues of zebrafish embryos exposed to test compounds would indicate whether the compounds are taken up by the tissue and therefore accessible to transporter proteins; (b) dye accumulation assays could be performed with other, structurally diverse fluorescent transporter substrates that bind to other binding sites in the protein, such as Hoechst 33342; and (c) knockout/knockdown of Abcb4 and of other, potentially relevant efflux transporters in zebrafish embryos, such as from the Abcc subfamily, could elucidate which transporters play roles for efflux of rhodamine B and other proxy dyes in the dye accumulation assay.

Acknowledgements

We like to thank Nicole Schwaiger for taking care of the zebrafish, for providing zebrafish eggs, for her support with the VAST system and for performing qPCR; Peggy Wellner for her help with the dye assays and for her support with culturing Sf9 cells, setting up the baculovirus system and performing ATPase assays; Dr. Elisabet Teixido Condomines for technical support and her kind help with the VAST and the KNIME workflow; Prof. Kai-Uwe Goss for his advice concerning physicochemical parameters of the test compounds; and Dr. Stephan Fischer for his help with QGene. FB was supported with a fellowship from the German Academic Exchange Service (Deutscher Akademischer Austauschdienst—DAAD, ALEARG program) and KBM with a fellowship from the German Federal Environmental Foundation (Deutsche Bundesstiftung Umwelt—DBU, https://www.dbu.de/2535.html). This work was part of the Integrated Project 'Exposome' of the topic 'Chemicals in the Environment' at the Helmholtz Centre for Environmental Research—UFZ.

Author contributions

FB, KBM, and TL designed the study. FB and SSch established the dye accumulation assay and FB performed the experiments. FB, CML, SSch, and TL analyzed the dye accumulation assay results and made the graphs. KBM and TL established the ATPase assays with recombinant zebrafish Abcb4. KBM performed the ATPase experiments, and KBM and TL analyzed the data and made the graphs. TL analyzed the qPCR data and made the graphs. FB, KBM, and TL wrote the paper, and CML and SSch commented on it. All authors approved the final version of the paper.

References

1 Luckenbach T and Epel D (2008) ABCB- and ABCC-type transporters confer multixenobiotic resistance and form an environment-tissue barrier in bivalve gills. *Am J Physiol Regul Integr Comp Physiol* **294**, R1919–R1929.
2 Bard SM (2000) Multixenobiotic resistance as a cellular defense mechanism in aquatic organisms. *Aquat Toxicol* **48**, 357–389.
3 Epel D, Luckenbach T, Stevenson CN, Macmanus-Spencer LA, Hamdoun A and Smital T (2008) Efflux transporters: newly appreciated roles in protection against pollutants. *Environ Sci Technol* **42**, 3914–3920.
4 Kurelec B (1992) The multixenobiotic resistance mechanism in aquatic organisms. *Crit Rev Toxicol* **22**, 23–43.
5 Ferreira M, Costa J and Reis-Henriques MA (2014) ABC transporters in fish species: a review. *Front Physiol* **5**, 266.
6 Luckenbach T, Fischer S and Sturm A (2014) Current advances on ABC drug transporters in fish. *Comp Biochem Physiol C Toxicol Pharmacol* **165**, 28–52.
7 Annilo T, Chen ZQ, Shulenin S, Costantino J, Thomas L, Lou H, Stefanov S and Dean M (2006) Evolution of the vertebrate ABC gene family: analysis of gene birth and death. *Genomics* **88**, 1–11.
8 Fischer S, Klüver N, Burkhardt-Medicke K, Pietsch M, Schmidt AM, Wellner P, Schirmer K and Luckenbach T (2013) Abcb4 acts as multixenobiotic transporter and active barrier against chemical uptake in zebrafish (*Danio rerio*) embryos. *BMC Biol* **11**, 69.
9 Fleming A, Diekmann H and Goldsmith P (2013) Functional characterisation of the maturation of the blood-brain barrier in larval zebrafish. *PLoS One* **8**, e77548.
10 Gordon WE, Espinoza JA, Leerberg DM, Yelon D and Hamdoun A (2019) Xenobiotic transporter activity in zebrafish embryo ionocytes. *Aquat Toxicol* **212**, 88–97.
11 Keiter S, Burkhardt-Medicke K, Wellner P, Kais B, Farber H, Skutlarek D, Engwall M, Braunbeck T, Keiter SH and Luckenbach T (2016) Does perfluorooctane sulfonate (PFOS) act as chemosensitizer in zebrafish embryos? *Sci Total Environ* **548–549**, 317–324.
12 Friche E, Skovsgaard T and Danø K (1988) Multidrug resistance: drug extrusion and its counteraction by chemosensitizers. *Eur J Haematol Suppl* **48**, 59–67.
13 Skovsgaard T, Dano K and Nissen NI (1984) Chemosensitizers counteracting acquired resistance to anthracyclines and vinca alkaloids in vivo. A new treatment principle. *Cancer Treat Rev* **11**(Suppl A), 63–72.
14 Smital T and Kurelec B (1998) The activity of multixenobiotic resistance mechanism determined by rhodamine B-efflux method as a biomarker of exposure. *Mar Environ Res* **46**, 443–447.
15 Smital T, Luckenbach T, Sauerborn R, Hamdoun AM, Vega RL and Epel D (2004) Emerging contaminants–pesticides, PPCPs, microbial degradation products and natural substances as inhibitors of multixenobiotic defense in aquatic organisms. *Mutat Res* **552**, 101–117.
16 Daughton CG and Ternes TA (1999) Pharmaceuticals and personal care products in the environment: agents of subtle change? *Environ Health Perspect* **107**(Suppl 6), 907–938.
17 Kurelec B, Smital T, Pivcevic B, Eufemia N and Epel D (2000) Multixenobiotic resistance, P-glycoprotein, and chemosensitizers. *Ecotoxicology* **9**, 307–327.
18 Cunha V, Burkhardt-Medicke K, Wellner P, Santos MM, Moradas-Ferreira P, Luckenbach T and Ferreira

M (2017) Effects of pharmaceuticals and personal care products (PPCPs) on multixenobiotic resistance (MXR) related efflux transporter activity in zebrafish (*Danio rerio*) embryos. *Ecotoxicol Environ Saf* **136**, 14–23.
19 Klaassen CD and Aleksunes LM (2010) Xenobiotic, bile acid, and cholesterol transporters: function and regulation. *Pharmacol Rev* **62**, 1–96.
20 Deeley RG, Westlake C and Cole SP (2006) Transmembrane transport of endo- and xenobiotics by mammalian ATP-binding cassette multidrug resistance proteins. *Physiol Rev* **86**, 849–899.
21 Burkhardt-Medicke K (2018) Studies on the interaction of chemicals with cellular efflux transporter proteins *Danio rerio* Abcb4 and Homo sapiens ABCB1. PhD thesis, TU Dresden.
22 Ambudkar SV, Lelong IH, Zhang J, Cardarelli CO, Gottesman MM and Pastan I (1992) Partial purification and reconstitution of the human multidrug-resistance pump: characterization of the drug-stimulatable ATP hydrolysis. *Proc Natl Acad Sci USA* **89**, 8472–8476.
23 Sharom FJ, Yu X and Doige CA (1993) Functional reconstitution of drug transport and ATPase activity in proteoliposomes containing partially purified P-glycoprotein. *J Biol Chem* **268**, 24197–24202.
24 Glavinas H, Mehn D, Jani M, Oosterhuis B, Heredi-Szabo K and Krajcsi P (2008) Utilization of membrane vesicle preparations to study drug-ABC transporter interactions. *Expert Opin Drug Metab Toxicol* **4**, 721–732.
25 Westerfield M (2000) The Zebrafish Book. A Guide for the Laboratory Use of Zebrafish (*Danio rerio*), 4th edn. University of Oregon Press, Eugene, OR.
26 Nagel R (2002) DarT: The embryo test with the Zebrafish *Danio rerio*–a general model in ecotoxicology and toxicology. *Altex* **19**(Suppl 1), 38–48.
27 OECD (2013) OECD guideline for the testin of chemcial 236 - Fish Embryo Acute Toxicity (FET) Test. Available at www.oecd-library.org https://www.oecd-ilibrary.org/environment/test-no-236-fish-embryo-acute-toxicity-fet-test_9789264203709-en Accessed December 1, 2020.
28 Muller PY, Janovjak H, Miserez AR and Dobbie Z (2002) Processing of gene expression data generated by quantitative real-time RT-PCR. *Biotechniques* **32**, 1372–1374, 1376, 1378–1379.
29 Simon P (2003) Q-Gene: processing quantitative real-time RT-PCR data. *Bioinformatics* **19**, 1439–1440.
30 Neyfakh AA (1988) Use of fluorescent dyes as molecular probes for the study of multidrug resistance. *Exp Cell Res* **174**, 168–176.
31 Svoboda KR, Linares AE and Ribera AB (2001) Activity regulates programmed cell death of zebrafish Rohon-Beard neurons. *Development* **128**, 3511–3520.
32 Berthold MR, Cebron N, Dill F, Gabriel TR, Kötter T, Meinl T, Ohl P, Sieb C, Thiel K and Wiswedel B (2007) KNIME: The Konstanz Information Miner. In Data Analysis, Machine Learning and Applications: Proceedings of the 31st Annual Conference of the Gesellschaft für Klassifikation eV, Albert-Ludwigs-Universität Freiburg, March 7–9, 2007 pp. 319–326. New York: Springer.
33 Tal T, Yaghoobi B and Lein PJ (2020) Translational toxicology in zebrafish. *Curr Opin Toxicol* **23–24**, 56–66.
34 Scholz S, Fischer S, Gündel U, Küster E, Luckenbach T and Voelker D (2008) The zebrafish embryo model in environmental risk assessment–applications beyond acute toxicity testing. *Environ Sci Pollut Res Int* **15**, 394–404.
35 MacRae CA and Peterson RT (2015) Zebrafish as tools for drug discovery. *Nat Rev Drug Discov* **14**, 721–731.
36 Carvalho L and Heisenberg CP (2010) The yolk syncytial layer in early zebrafish development. *Trends Cell Biol* **20**, 586–592.
37 Frank NY, Margaryan A, Huang Y, Schatton T, Waaga-Gasser AM, Gasser M, Sayegh MH, Sadee W and Frank MH (2005) ABCB5-mediated doxorubicin transport and chemoresistance in human malignant melanoma. *Cancer Res* **65**, 4320–4333.
38 Sarkadi B, Price EM, Boucher RC, Germann UA and Scarborough GA (1992) Expression of the human multidrug resistance cDNA in insect cells generates a high activity drug-stimulated membrane ATPase. *J Biol Chem* **267**, 4854–4858.
39 Pouliot JF, L'Heureux F, Liu Z, Prichard RK and Georges E (1997) Reversal of P-glycoprotein-associated multidrug resistance by ivermectin. *Biochem Pharmacol* **53**, 17–25.
40 Polli JW, Wring SA, Humphreys JE, Huang L, Morgan JB, Webster LO and Serabjit-Singh CS (2001) Rational use of in vitro P-glycoprotein assays in drug discovery. *J Pharmacol Exp Ther* **299**, 620–628.
41 Callegari E, Malhotra B, Bungay PJ, Webster R, Fenner KS, Kempshall S, LaPerle JL, Michel MC and Kay GG (2011) A comprehensive non-clinical evaluation of the CNS penetration potential of antimuscarinic agents for the treatment of overactive bladder. *Br J Clin Pharmacol* **72**, 235–246.
42 Schinkel AH, Smit JJ, van Tellingen O, Beijnen JH, Wagenaar E, van Deemter L, Mol CA, van der Valk MA, Robanus-Maandag EC, te Riele HP *et al.* (1994) Disruption of the mouse mdr1a P-glycoprotein gene leads to a deficiency in the blood-brain barrier and to increased sensitivity to drugs. *Cell* **77**, 491–502.
43 Feng B, Mills JB, Davidson RE, Mireles RJ, Janiszewski JS, Troutman MD and de Morais SM (2008) In vitro P-glycoprotein assays to predict the in vivo interactions of P-glycoprotein with drugs in the central nervous system. *Drug Metab Dispos* **36**, 268–275.

44 Loncar J, Popovic M, Krznar P, Zaja R and Smital T (2016) The first characterization of multidrug and toxin extrusion (MATE/SLC47) proteins in zebrafish (*Danio rerio*). *Sci Rep* **6**, 28937.
45 Long Y, Li Q, Zhong S, Wang Y and Cui Z (2011) Molecular characterization and functions of zebrafish ABCC2 in cellular efflux of heavy metals. *Comp Biochem Physiol C Toxicol Pharmacol* **153**, 381–391.
46 Long Y, Li Q, Li J and Cui Z (2011) Molecular analysis, developmental function and heavy metal-induced expression of ABCC5 in zebrafish. *Comp Biochem Physiol B Biochem Mol Biol* **158**, 46–55.
47 Yin H, Bai P, Miao P, Chen M, Hu J, Deng X and Yin J (2016) Functional expressions of adenosine triphosphate-binding cassette transporters during the development of zebrafish embryos and their effects on the detoxification of cadmium chloride and betanaphthoflavone. *J Appl Toxicol* **36**, 925–935.
48 Shapiro AB and Ling V (1998) The mechanism of ATP-dependent multidrug transport by P-glycoprotein. *Acta Physiol Scand Suppl* **643**, 227–234.
49 Orlowski S, Mir LM, Belehradek J Jr and Garrigos M (1996) Effects of steroids and verapamil on P-glycoprotein ATPase activity: progesterone, desoxycorticosterone, corticosterone and verapamil are mutually non-exclusive modulators. *Biochem J* **317**(Pt 2), 515–522.
50 Litman T, Zeuthen T, Skovsgaard T and Stein WD (1997) Structure-activity relationships of P-glycoprotein interacting drugs: kinetic characterization of their effects on ATPase activity. *Biochim Biophys Acta* **1361**, 159–168.
51 Chufan EE, Kapoor K, Sim HM, Singh S, Talele TT, Durell SR and Ambudkar SV (2013) Multiple transport-active binding sites are available for a single substrate on human P-glycoprotein (ABCB1). *PLoS One* **8**, e82463.
52 Aller SG, Yu J, Ward A, Weng Y, Chittaboina S, Zhuo R, Harrell PM, Trinh YT, Zhang Q, Urbatsch IL *et al.* (2009) Structure of P-glycoprotein reveals a molecular basis for poly-specific drug binding. *Science* **323**, 1718–1722.
53 Dobson PD and Kell DB (2008) Carrier-mediated cellular uptake of pharmaceutical drugs: an exception or the rule? *Nat Rev Drug Discov* **7**, 205–220.
54 EPA, U. (2012) Estimation Programs Interface Suite™ for Microsoft® Windows, v 4.11. United States Environmental Protection Agency, Washington, DC.

Supporting information

Additional supporting information may be found online in the Supporting Information section at the end of the article.

Fig. S1. Illustration of the automatic image analysis with a KNIME workflow.

Fig. S2. Fluorescence levels in zebrafish embryos are sensitive to compound treatment.

Fig. S3. Rhodamine B accumulation in zebrafish embryos over time.

Fig. S4. Rhodamine B washout experiments.

Table S1. (A-C) Data related to qPCR for expression analysis of *abcb4* and *abcb5* in 72 hpf zebrafish embryos.